A Sentinel-1-based clustering analysis for geo-hazards mitigation at regional scale: a case study in Central Italy

Roberto Montalti, Lorenzo Solari, Silvia Bianchini, Matteo Del Soldato, Federico Raspini & Nicola Casagli

Published online: 25 Nov 2019.

Submit your article to this journal 🗗

View related articles 🗗

View Crossmark data 🗗

Taylor & Francis
Taylor & Francis Group

🔓 OPEN ACCESS | Check for updates

A Sentinel-1-based clustering analysis for geo-hazards mitigation at regional scale: a case study in Central Italy

Roberto Montalti, Lorenzo Solari* (ID), Silvia Bianchini (ID), Matteo Del Soldato (ID), Federico Raspini and Nicola Casagli (ID)

Department of Earth Science, University of Florence, Florence, Italy

ABSTRACT

In the last decade satellite remote sensing has become an effective tool for monitoring geo-hazard-induced ground motions, and has been increasingly used by the scientific community. Direct and indirect costs due to geo-hazards are currently rising, causing serious socio-economics and casualty losses. Therefore, creating a priority list turns out to be essential to highlight the most relevant ground deformations and to better focus risk management practices at regional scale. The Sentinel-1 constellation, thanks to the 6-days repeatability and the free availability of the data, allows to easily update the geo-hazard-induced ground motions, compared to other kind of satellite sensors. In this work, a hot-spot-like method is presented by filtering a large stack of Sentinel-1 images processed by means of the SqueeSAR algorithm. Three periods, with six months repetitiveness, have been analysed in order to evaluate the behaviour and evolution of deformation clusters. The target area is Tuscany Region, located in the central part of Italy and affected by a wide gamma of geohazards, ranging from landslides to large subsidence areas. The final output is a geo-database of ground motions that can be used by regional authorities to prioritize and to effectively plan local risk reduction actions.

1. Introduction

Ground deformations, such as land subsidence and landslides, induced by natural processes or human activities entail severe damages, in terms of human and economic losses in Europe and worldwide, with direct and indirect costs for more than 1$billion year (Hu et al. 2002; Del Soldato et al. 2017; Herrera et al. 2018). Uncontrolled urbanization has enhanced human influence on the natural environment, leading to an increased exposure of the population to different geohazards. Among them, landslides play a key role causing serious socio-economics and casualty

CONTACT Roberto Montalti ✉ roberto.montalti@unifi.it; roberto.montalti90@gmail.com
*Centre Tecnològic de Telecomunicacions de Catalunya (CTTC), Division of Geomatics, Av. Gauss, 7 E-08860 Castelldefels (Barcelona, Spain)

losses. For example, in Europe, a report of the European Environment Agency states that landslides caused 312 fatalities and a total direct and indirect cost of €48 billion between 1998 and 2009 (Spizzichino et al. 2010; Herrera et al. 2018). Subsidence is commonly referred to a gentle and graduate lowering or to a sudden sinking of the ground surface (Galloway and Burbey 2011). Subsidence can be triggered by several kind of factors, such as ground water and natural gas extraction, compaction of fine-grained sediments due to load imposition and underground mining activity (Herrera et al. 2012). Usually, subsidence is a major threat in urban areas, especially for linear infrastructures, such us bridges, roads and railways, caused by the continuous ground lowering over time, and leads to relevant damage especially when differential settlements occur (Solari et al. 2018b). In this case, the derived economic loss is not negligible. Hu et al. (2004) determined that in China 45 cities recorded severe subsidence, causing a total economic loss of around $100 million/year. Faunt et al. (2016) reported that, between 1955 and 1972, the total cost of subsidence due to water withdrawal reached $1.3 billion of damages only for California (United States).

Since '90 s, Earth observation techniques exploiting SAR (Synthetic Aperture Radar) images have been used in several fields of the natural sciences, but only in the last twenty years the technological advances allowed the scientists to effectively study landslides and geo-hazards in general (Massonnet and Feigl 1998; Bianchini et al. 2012; Tofani et al. 2013). The development of Multi Temporal Interferometric SAR (MTInSAR) has improved and extended the applications of interferometric techniques for geo-hazards monitoring and mapping (Bianchini et al. 2017), providing not only scientific products, but operative information for Civil Protection purposes and for regional and national authorities in charge of hydrogeological risk management, as well.

The launch of the Sentinel-1 constellation, composed by two twin satellites (Sentinel-1A and Sentinel-1B) designed by Europe Space Agency (ESA), ensures a systematic and regular acquisition plan of radar images, by providing free data every six days. (Torres et al. 2012). Sentinel-1 operates in several acquisition modes; for geo-hazards detection the "Interferometric Wide Swath", with a 250 km wide swath and 5x20 m ground resolution, is commonly used (Aschbacherand Milagro-Pérez 2012). Sentinel-1 data supports several applications as testified by a large number of studies, such as landslide detection, mapping and characterization (Barra et al. 2016; Intrieri et al. 2018; Del Soldato et al. 2018b; Solari et al. 2018c), landslides monitoring (Dai et al. 2016; Raspini et al. 2018); mining activity (Abdikan et al. 2016; Ng et al. 2017; Zhang et al. 2018), subsidence phenomena (Sowter et al. 2016; van der Horst et al. 2018) and earthquakes (Plank 2014; Wang et al. 2017; Vajedian et al. 2018).

In this work, the regional-scale image capability of Sentinel-1 constellation has been exploited for detecting and mapping active moving areas. Three different temporal baselines have been analysed for evaluating the spatial evolution and multi-temporal variations of the areas, in order to highlight the most representative ground deformations at regional scale and to track their evolution. The study area is the Tuscany Region, located in Central Italy and characterized by an extremely variegated landscape. The methodology exploits radar images processed by means of SqueeSAR algorithm to create a new geodatabase of moving areas at regional scale in Tuscany

Region, useful not only from a scientific point view, but for risk management and Civil Protection purposes, as well.

## 2. Geographical and geomorphological setting of tuscany region

The Tuscany Region is located in central Italy and extends up about 22.994 km². It is administratively subdivided into 279 municipalities and 10 provinces: Arezzo (AR), Siena (SI), Grosseto (GR), Pisa (PI), Livorno (LI), Massa-Carra (MC), Pistoia (PT), Prato (PR) and Lucca (LU). Furthermore, the Tuscan territory includes an island archipelago composed by six main islands and other small ones. The regional capital is Florence, the most populated city, with about 380.000 inhabitants.

Tuscany Region presents an extremely variegated landscape. Mountains cover 25.1% of the region from NW to SE along the Apennines, where mountain heights can be higher than 2000 meters a.s.l. (the highest Monte Prado, 2054 meters a.s.l.). The central part of the territory is mainly characterized by hills (66.5%) and flat areas (8.4%), as well as by wide valleys where the main rivers flow (Figure 1(a)).

From the climatic point of view, the region is generally Mediterranean, with hot and dry summers and moist and mild winters (Csa as in the Köppen-Geiger classification) (Peel et al. 2007), even if it locally can vary according to the position of orographic elements and along the coast. Froma rainfall point of view, there are two precipitation peaks: the main one during the autumn period, the second one during the winter or the spring period. Summer is the driest season of the year (Rapetti and Vittorini 1994). The major rainfall events are located along the Apennines, especially in the NW part, with mean annual peaks up to 2000 mm/year in Apuan Alps. Instead, the lower rainfall values are typical in the southern Tuscany, with mean annual peaks lower than 600 mm/yr (Rapetti and Vittorini 1994; Rosi et al. 2012).

Froma geological point of view, Tuscany Region belongs to the Northern Apennine. The geological setting is characterized by an overlapping of three main geological units: Ligurian, Tuscanian and Umbro-Marchigian units. The Apennines are one of the youngest mountain chains in the world, formed during the Neogene and Quaternario. Active tectonic makes Apenninic area prone to several geological hazards such as earthquakes and slope instability (Bortolotti 1992; Vai and Martini 2013).

Tuscany Region is characterized by various geological and topographic patterns; thus, geo-hazards are heterogeneously distributed throughout the territory. Figure 1b shows the spatial distribution of typical phenomena observable by radar satellite, such as landslides and subsidence. In this work, we used the landslides database published by Rosi et al. (2018), based on the improvement of Italian Landslides Inventory (IFFI) project, produced by the Institute for Environmental Protection and Research (ISPRA). In this database 117.000 landslides are mapped and classified according to their state of activity; 22% of them are classified as "active", 74% as "dormant" and 4% as "stabilised". Rosi et al. (2016) derived a subsidence database for the Tuscany Region, on the basis of ERS 1/2 and Envisat interferometric products. This database is composed of 13 main zones, with a total area of 2035 km², equals to 9% of the Tuscany surface. Figure 1b shows the distribution of landslides or/and subsidence for
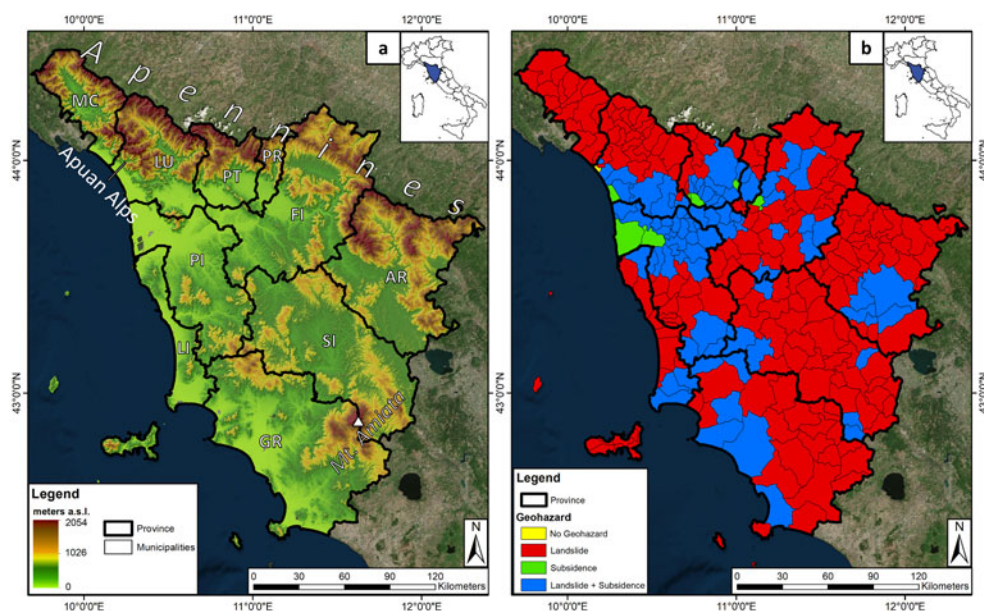
Figure 1. Geographical characterization and Digital Elevation Model (DEM) of Tuscany Region (a) and spatial distribution of geohazard observable by satellite radar data (b). Source: Author

each municipality. The 69% of the municipalities includes mapped landslides, while the 28% records both landslides and known subsidence areas and only 0.4% of them register no-known geohazards (i.e. 1 among279 municipalities). These data confirm the need and importance of a priority list to manage geo-risks in an effective way.

3. Data and method

The goal of the methodology is to highlight the most relevant ground deformations in Tuscany Region, by means of satellite radar interferometry and using simple GIS (Geographical Information System) tools, making an analysis from April 2017 to April 2018 subdivided into three periods. The workflow is conceived to be reproducible and fast to apply, providing a geodatabase that contains interferometric and qualitative parameters, concerning the hydrogeological phenomena.

The methodology is subdivided into three main steps:

1. deformation map generation;
2. active moving areas extraction;
3. cluster classification and persistence analysis.

3.1. Deformation maps generation

We used Sentinel-1A and Sentinel-1B images from October 2014 to April 2017, to create the first deformation map, as baseline of our analysis, by means of SqueeSAR algorithm (Ferretti et al. 2011). After that, other two deformation maps were obtained, i.e. from October 2014 to October 2017, and from October 2014 to April

Table 1. InSAR database.

Period	Dates	Constellation	Geometry	Number of images
1°	October2014–April 2017	Sentinel-1A and Sentinel-1B	Ascending	70
			Descending	68
2°	October 2014–April 2017		Ascending	99
			Descending	96
3°	October 2014–April 2017		Ascending	130
			Descending	126

2018, in order to update the results every six months and highlight the evolution of the hydrogeological phenomena (Table 1).

The SqueeSAR algorithm represents the evolution of the Permanent Scatterer SAR Interferometry (PSInSAR) (Ferretti et al. 2001), which aimed at identifying radiometrically stable reflectors called Permanent Scatterers (PS), by exploiting the whole stack of SAR images. Every PS represents a pixel of a SAR image with high signal coherence, mainly corresponding to rock outcrops and man-made objects. The main drawback of this technique is the low density of PS that could be obtained in agricultural and peri-urban areas ($< 10 \, \mathrm{PS/km^2}$ using C-band radar images), compared to the PS density in urban areas ($> 100 \, \mathrm{PS/km^2}$ using C-band radar images).

The SqueeSAR algorithm was designed to overcome this limitation, defining a new type of PS points: the Distributed Scatterers (DS). A DS is a target corresponding to an area, where a certain number of neighbouring pixels shares similar reflectivity values and moderate interferometric coherence. By combining and merging the signal of these pixels, it is possible to extract a point-like feature with high interferometric coherence. DS typically match with homogeneous areas such as deserts, debris areas or uncultivated area. The SqueeSAR approach jointly processes PS and DS, considering their different statistical behaviour. This is possible thanks to a space adaptive filtering, DespecKS (Ferretti et al. 2011), that is able to statistically average homogeneous pixels (SHP) preserving the information of point-wise associated to point targets. The filter is based on Kolmogorov-Smirnov statistical test (Stephens 1970; Kvam and Vidakovic 2007). Basically, for every image-pixel, this kind of statistical test is applied to all the pixels within a certain estimation window, centred on the pixel under analysis to select SHP families (Ferretti et al. 2011). After that, it is possible (1) to despeckle amplitude data; (2) to filter interferometric phase values; (3) to estimate coherence values properly.

3.2. Active moving areas extraction

Extracting deformation maps from Multi-temporal InSAR technique represents a good starting point to highlight possible relevant zones affected by hydrogeological risk. In this work, we derived active moving areas using a simple hot-spot-like method in GIS environment, already followed by other authors (Barra et al. 2017; Solari et al. 2018a), divided into two main steps:

- Velocity filtering: PS and DS points were filtered with a velocity threshold of ±7,5 mm/year. This value is equal to three times the standard deviation of the

velocity values of both datasets. This value has been chosen to extract just the most representative points for "fast" moving areas at regional scale.

- Cluster extraction: the resulting filtered map was further analysed to derive the final moving areas. This product was obtained by buffering PS/DS. We choose a buffer size of 100 meters and a cluster size with minimum three PS. We chose this buffer size and cluster size based on our knowledge, defining the common size of a landslide in the Tuscany Region. Each cluster is characterized by a value of mean velocity, mean standard deviation and mean coherence of the time series of PS/DS points composing the clusters.

3.3. Cluster classification and persistence analysis

The classification of each cluster is based on radar interpretation, as firstly defined by Farina et al. (2007), introducing the PSI analysis cross-compared with ancillary data, such as geology, geomorphology, multi-temporal orthophotos, regional technical maps. For every type of geohazard the following databases were used:

- for landslides (La) phenomena, the IFFI inventory improved with ERS 1/2 and Envisat interferometric data (Rosi et al. 2018);
- for subsidence (Su) and uplift (Up) phenomena, the inventory published by Rosi et al. (2016);
- for deformations due to geothermal activity (GA), the geothermal inventory of Tuscany Region and
- for deformations due to mining activity (MA), the mining inventory of Tuscany Region.

Furthermore, the three periods were analysed to highlight possible temporal and geometric persistence areas (TGPA) among clusters. A TGPA is defined when clusters of moving points, which are present in each period and acquisition geometry, overlap each other. TPGAs represent the most enduring and representative ground deformations, thus they are useful to highlight the most relevant situations that have to be prioritized.

4. Results

In this chapter, the results obtained by following the methodology are presented. Some examples of active moving areas will be presented as well.

4.1. Deformation maps

The first step of the methodology is devoted to the generation of three deformation maps performing a SqueeSAR analysis of Sentinel-1 images. Figure 2a,b shows the deformation maps regarding the first period (October 2014–April 2017), representing the starting point for the multi-temporal comparison of deformation clusters. These maps offer a great wealth of information on ground velocity distribution and they
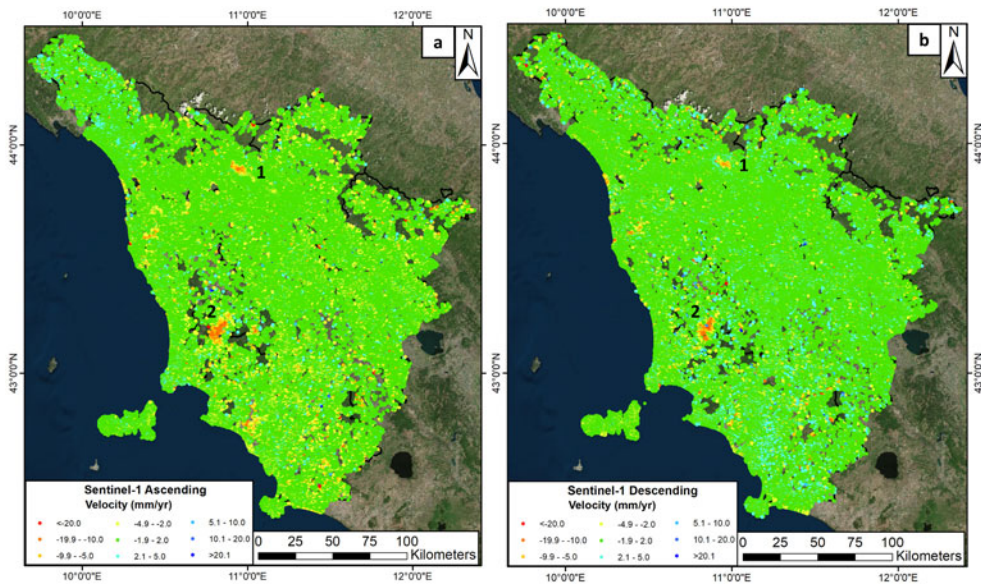
Figure 2. Deformation map in ascending geometry (a) and descending geometry (b) from October 2014 to April 2017 using SqueeSAR algorithm. (1) Firenze-Prato-Pistoia basin, (2) Larderello-Travale area. Source: Author

Table 2. Statistics of deformation maps. 1° period: October 2014 to April 2017, 2° period: October 2014 to October 2017, 3° period: October 2014 to April 2018.

Period	Geometry	Images	PS/DS	Velocity (mm/yr)			Mean coherence
				Min	Mean	Max	
1°	Asc	70	858.000	−63	0.9	26	0.89
1°	Desc	68	855.000	−104	0.87	43	0.91
2°	Asc	99	863.000	−77	0.95	22	0.9
2°	Desc	96	861.000	−43	0.92	43	0.9
3°	Asc	130	860.000	−65	1.2	21	0.9
3°	Desc	126	859.000	−39	1.1	34	0.88

can be used to highlight the most unstable areas at regional scale. It is possible to observe two main areas in red (representing points with negative velocities, i.e. movements away from the sensor), the first one located in northern Tuscany and the biggest one in the south-western part. These areas are well-known in scientific environment, both referred to subsidence phenomena: the first one along the Firenze-Prato-Pistoia basin (Colombo et al. 2003; Del Soldato et al. 2018b) and the second one in the Larderello-Travale area where geothermal activities take place (Batini et al. 2003), producing relevant subsidence effects (Manzella et al. 2018). In the same way, it is possible to observe the presence of PS/DS points probably attributable to landslides phenomena, both in the Apennine area and in the southern part of the Tuscany Region.

Table 2 shows the information about PS data of the three analysed periods. The deformation maps were obtained starting from a minimum of 68/70 radar images for the first period (October 2014–April 2017) to a maximum of 126/130 images for the last period (October 2014–April 2018). The number of PS/DS extracted is between

Table 3. Statistics for filtered deformation maps. 1° period: October 2014 to April 2016, 2° period: October 2014 to October 2017, 3° period: October 2014 to April 2018.

| Period	Geometry	PS/DS	Clusters	Overlapping percentage
1°	Asc	5.818	127	50
2°	Asc	5.490	94	
3°	Asc	4.328	86	
1°	Desc	5.694	120	62
2°	Desc	5.113	123	
3°	Desc	4.845	102	

855.000 and 863.000, with a mean density of 33 points/km². This latter parameter turns out to be maximum in urban areas, while minimum or equal to zero in cultivated areas and forested Apennine areas.

4.2. Active moving areas extraction

Once the deformation maps are obtained, it is possible to extract the active moving areas as described in Section 3.2. After applying the velocity filtering equal to ± 7.5 mm/yr, the PS/DS number is decreased by 99% in all the acquisition periods and geometries. In Table 3 the statistics about clusters extraction are summarised. "PS/DS" column indicates the number of remaining points after velocity filtering; this number decreases from the first period to the third one, with a maximum of 5.818 points in the first one, and a minimum of 4.328 points in the third one. This is due to a reduction of the general noise level of the datasets connected to the increase of the number of radar images analysed that grants an improvement of the accuracy of the results and of the velocity estimation. Consequently, the number of single points, that could represent false positive, is reduced. In the same way, clusters extracted from the deformation maps decrease from the first period to third one as well, with a minimum of 86 in the 3° period, to a maximum of 127 in the first period. The percentage of clusters overlapping in different periods is equal to 50% in ascending geometry and 62% in descending orbit.

4.3. Clusters classification

Following the last step of the methodology, the deformation clusters are classified on the basis of their triggering factor. Figure 3 shows the classification and position of the clusters and TGPA. The clusters due to landslides are located especially in the mountain areas (88%) along the Apennine chain and near Mt. Amiata. The landslide cluster with the highest PS/DS density is located in the municipality of Cavriglia (Arezzo province), shows a maximum number of PS/DS points of 210 in the second period and a minimum of 90 in the third period, over an area of 1.6 km². The maximum LOS velocity recorded is equal to 24 mm/yr. The 100% of the clusters due to geothermal activity are located in Larderello-Travale area, which is the most ancient exploited geothermal field in the world (Batini et al. 2003). The clusters due to subsidence phenomena are mainly found in the Pisa and Livorno provinces, with a percentage equal to 60% of the total. They are mainly located in agricultural areas, likely due to the exploitation of groundwater, and in harbour areas, related to sediment
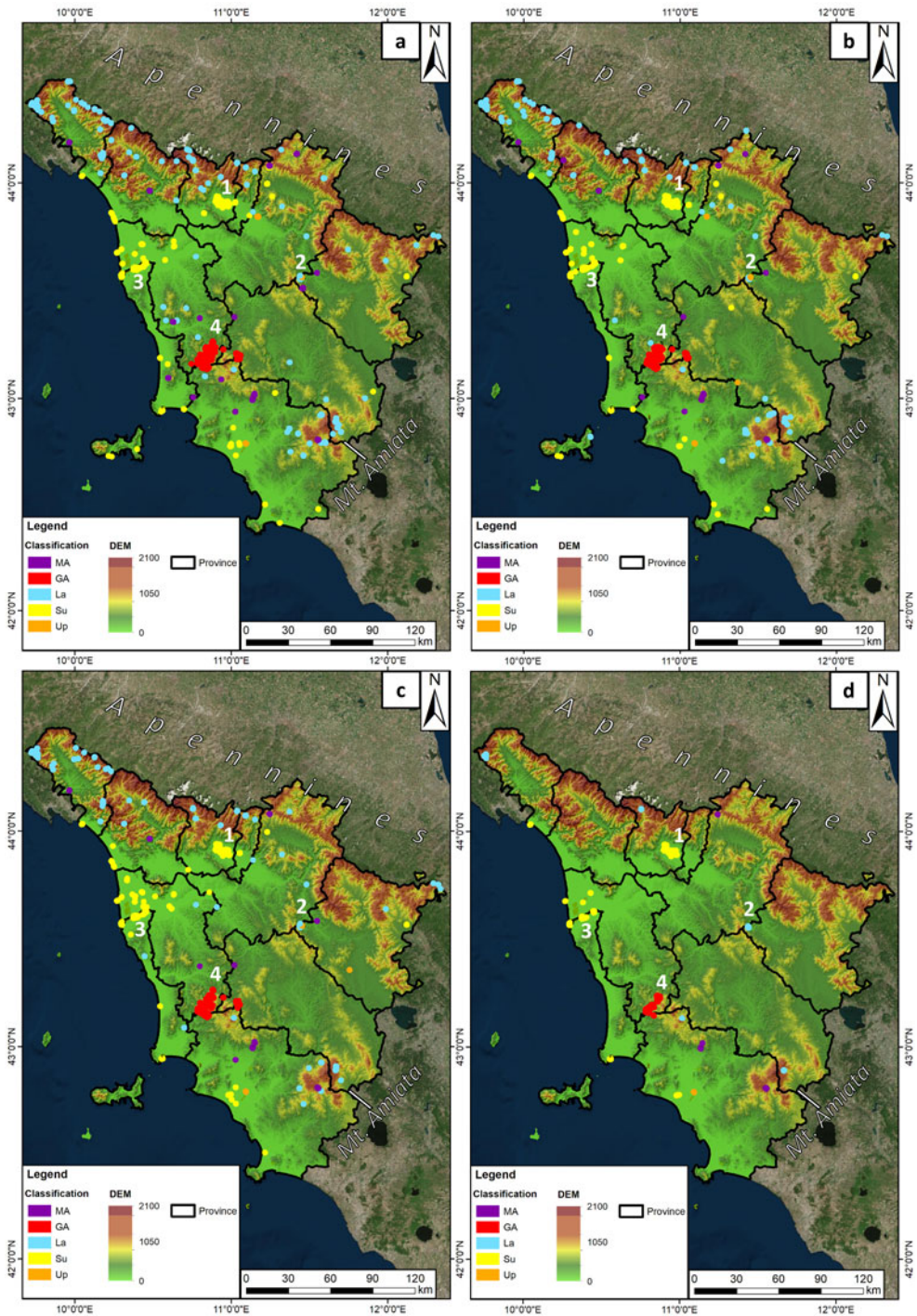
Figure 3. Cluster classification and TGPA maps. a): 1° period (October 2014 – April 2017); b): 2° period (October 2014 – October 2017); c): 3° period (October 2014 – April 2018); d): Temporal and Geometric Persistent Areas. GA: Geothermal Activity; La: Landslide; Su: Subsidence; MA: Mining Activity; Up: Uplift. (1) Firenze-Prato-Pistoia basin; (2) Cavriglia's landslide; (3) Livorno freight terminal and (4) Larderello-Travale area. Source: Author.
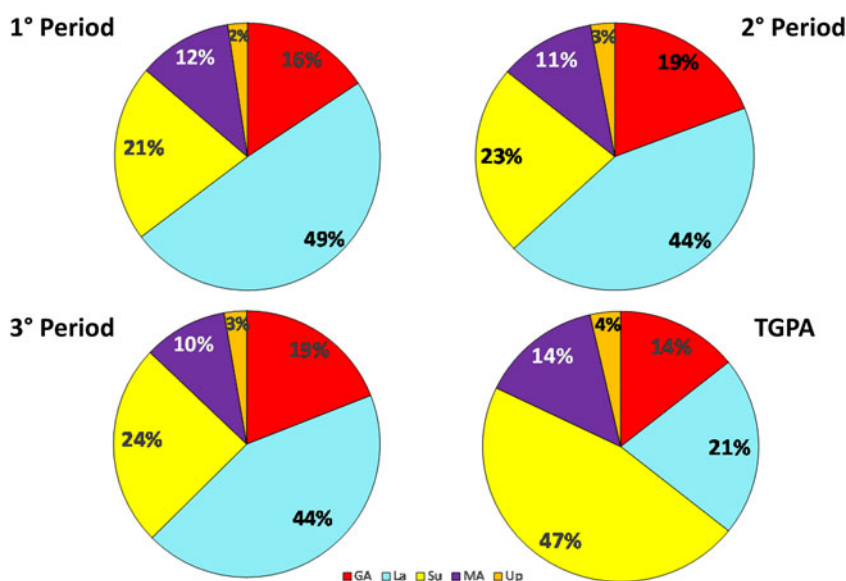
Figure 4. Classification statistics of the clusters in TR during the 1° period (October 2014–April 2017), 2° period (October 2014–October 2017), 3° period (October 2014–April 2018) and Temporally and Geometric Persistent Areas. GA: Geothermal Activity; La: Landslide; Su: Subsidence; MA: Mining Activity; Up: Uplift. Source: Author.

compaction. In this zone, the main group of clusters, with an area of 9 km², affects the structures of the Livorno freight terminal, started to be built in 2000, and composed by heavy facilities, such as warehouses and commercial areas. The subsidence probably depends on the consolidation process of compressible soils induced by the construction of heavy buildings. LOS velocities reach the maximum rate of 40 mm/yr. Another interesting and relevant group of subsidence clusters is situated along Firenze-Prato-Pistoia basin. This group is composed of five clusters covering a total area of 44 km² during the first period. The number of PS/DS points forming the clusters decreases along the time, therefore also their areal distribution decreases, reaching 39 km² in the third monitored period (October 2014–April 2018). LOS velocities recorded a little variation of few mm/yr, with maximum subsidence rates decreasing from 21 mm/yr to 18 mm/yr.

Figure 4 shows the temporal evolution of moving areas over Tuscany Region and their classification. The results indicate a homogeneous percentage among geohazard, with the landslides as the most occurring phenomenon, followed by the subsidence and the geothermal activity. On the other hand, the most common triggering cause for TPGA is subsidence (47%), followed by landslides (21%) and geothermal activity (14%). The percentage of landslides is reduced by more than a half considering the first and the last monitoring period, whereas the percentage of subsidence-related clusters is doubled. This is due to three main factors: (i) in general, the subsidence has a deformation velocity more linear and regular than a movement caused by a landslide, and with a lower spatial and temporal variability; (ii) subsidence phenomena are located in flat areas, which are not subjected to typical radar distortions, such as foreshortening, layover and shadowing. Sometimes from a slope, on the basis of its
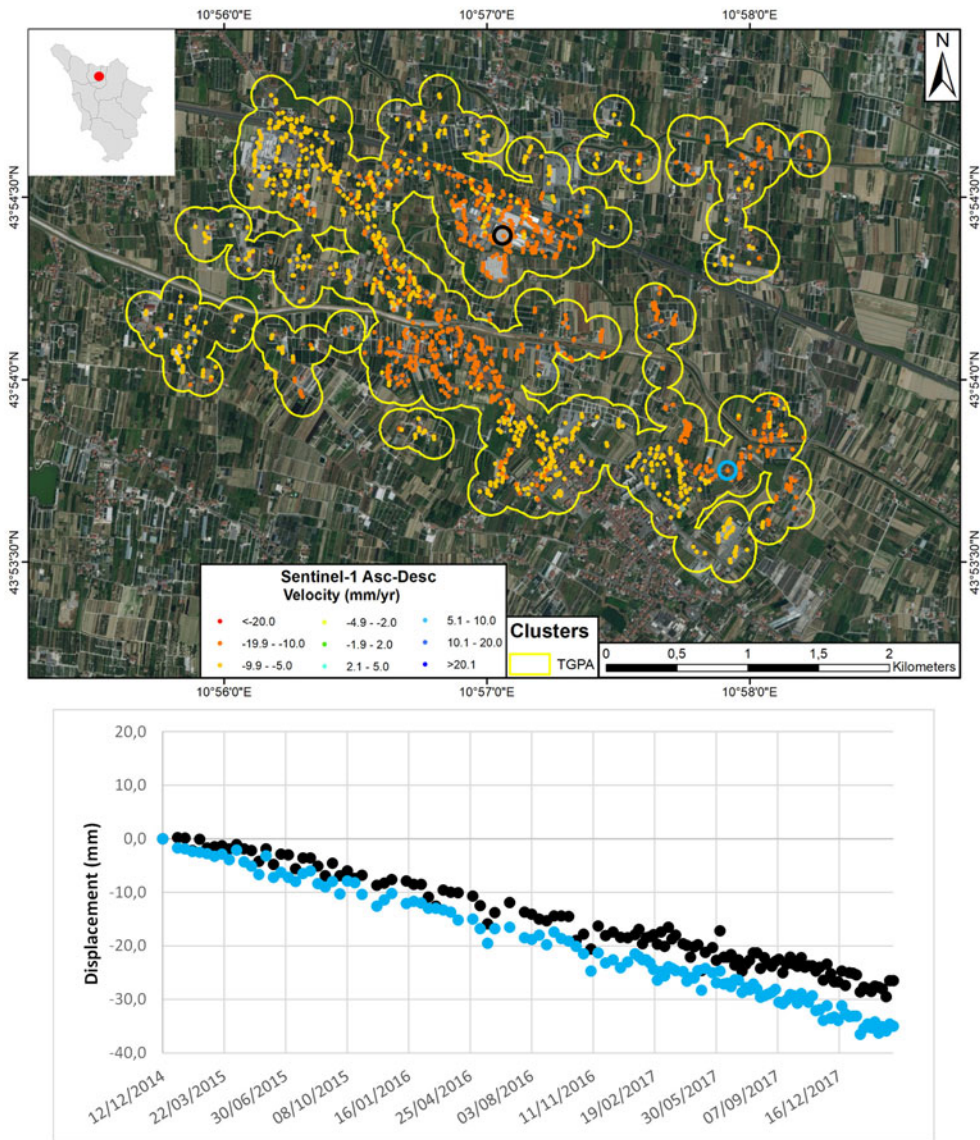
Figure 5. Example of TGPA in Pistoia - Prato - Firenze basin affected by subsidence phenomena. The PS/DS data correspond to the period from October 2014 to April 2018. The black, blue, green and red circles indicate the PS points from which time series were extracted. Source: Author

aspect, it can be easier to extract data in ascending geometry, rather than in descending geometry and vice versa, with differences in terms of PS/DS density and velocity; (iii) landslide phenomena are connected with rainfall, therefore during periods with low rainfall rates, the landslide velocity could fall below the used threshold.

Figure 5 presents an example of TGPA, related to subsidence due to water overexploitation, located in the plain between the cities of Prato and Pistoia, in the central portion of the Firenze-Prato-Pistoia basin. The Firenze-Prato-Pistoia basin has an extension of approximately 824 km2 and a mean elevation of ca. 50 m a.s.l. The plain

is crossed by the Ombrone creek in the Pistoia area, by the Bisenzio River in the Prato province and by the Arno River in the Florence area. The plain has an oblong shape in the NW–SE direction and is approximately 35 km wide and 100 km long (Del Soldato et al. 2018b). By the geological point of view, this plain is an intermountain valley formed during the late extensional phase of the formation of the northern Apennines and later filled with alluvial deposits, reaching a thickness of hundreds of meters. The shape is defined by normal faults in the NO flank, forming a semi-graben filled by a significant thickness of marshy-lacustrine sediments (Capecchi et al. 1975). The hydrogeological setting of the area is characterised by several confined aquifers situated at different depth, composed by clay lenses where water is extracted. Such aquifers supply the municipal aqueducts, the textile industries as well as trees and flowers nurseries that characterize the economical importance of this area. The aquifers were overexploited for more than thirty years, creating large subsidence bowl already detected by means of ERS 1/2 and Envisat interferometric products (Colombo et al. 2003; Del Soldato et al. 2018b). The TGPA (12 km^2) is composed by an average of 1756 PS/DS in the first period, 1730 for the second one, 1717 for the last one. The velocity analysis shows that the mean velocity is equal to 10.4 mm/yr and the maximum 19.3 mm/yr; for the second one the mean velocity is 10.1 mm/yr and the maximum 21 mm/yr; for the last one a mean velocity of 9.9 mm/yr and the maximum of 17.2 mm/yr. The time series of deformation show a linear and constant motion over the whole investigated period, the series shown in Figure 5 is an example.

Figure 6 shows an example of TGPA related to a landslide motion in the municipality of Abbadia San Salvatore located in the Siena province along the eastern flank of the Amiata Mountain (1780 a.s.l.), a Middle-Late Pleistocene volcano. Froma geological point of view, Amiata Mountain is characterized by a superimposition of different tectono-stratigraphic units, through the action of low-angle normal faults of different ages. The geological setting is subdivided from the bottom to the top as follows: the Tuscan Nappe succession (Late Triassic), the Ligurian Complex (Middle Jurassic – Olocene), the sediments of Radicofani basin (Early-Middle Pliocene), the magmatic complex (300 ka) Calamai et al. (1970), Gianelli et al. (1988),and Brogi (2008). According to the study of Coltorti et al. (2011), Abbadia San Salvatore and the eastern flank of the Volcano are characterized by a deep-seated gravitational slope deformation (DSGSD), subdivided in a deeper part with an activity difficult to verify and an active shallower part. The TGPA (500 m^2), located in the northern part of the municipality, is composed by 99 PS/DS in the first period, whit a maximum velocity of 24 mm/yr and a mean velocity of 14 mm/yr. The second period has a total of 79 PS/DS with a maximum velocity of 19 mm/yr and a mean velocity of 12.1 mm/yr. The last one has 67 PS/DS, with a maximum velocity of 18 mm/yr and a mean velocity of 11.7 mm/yr. The motion is linear through the whole monitored period in both orbits, as testified by the time series shown in Figure 6.
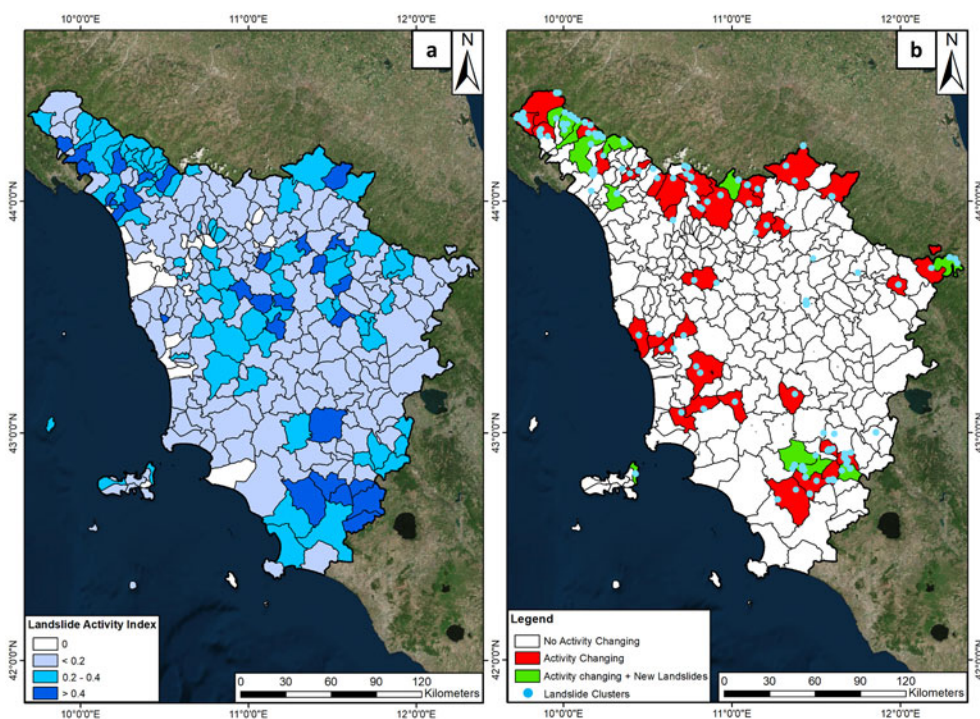
4.4. Update of the landslide's state of activity

The cluster database can be a reliable tool for checking landslide's State of Activity (SoA). In Figure 7a the municipalities map is shown, classified on the basis of the
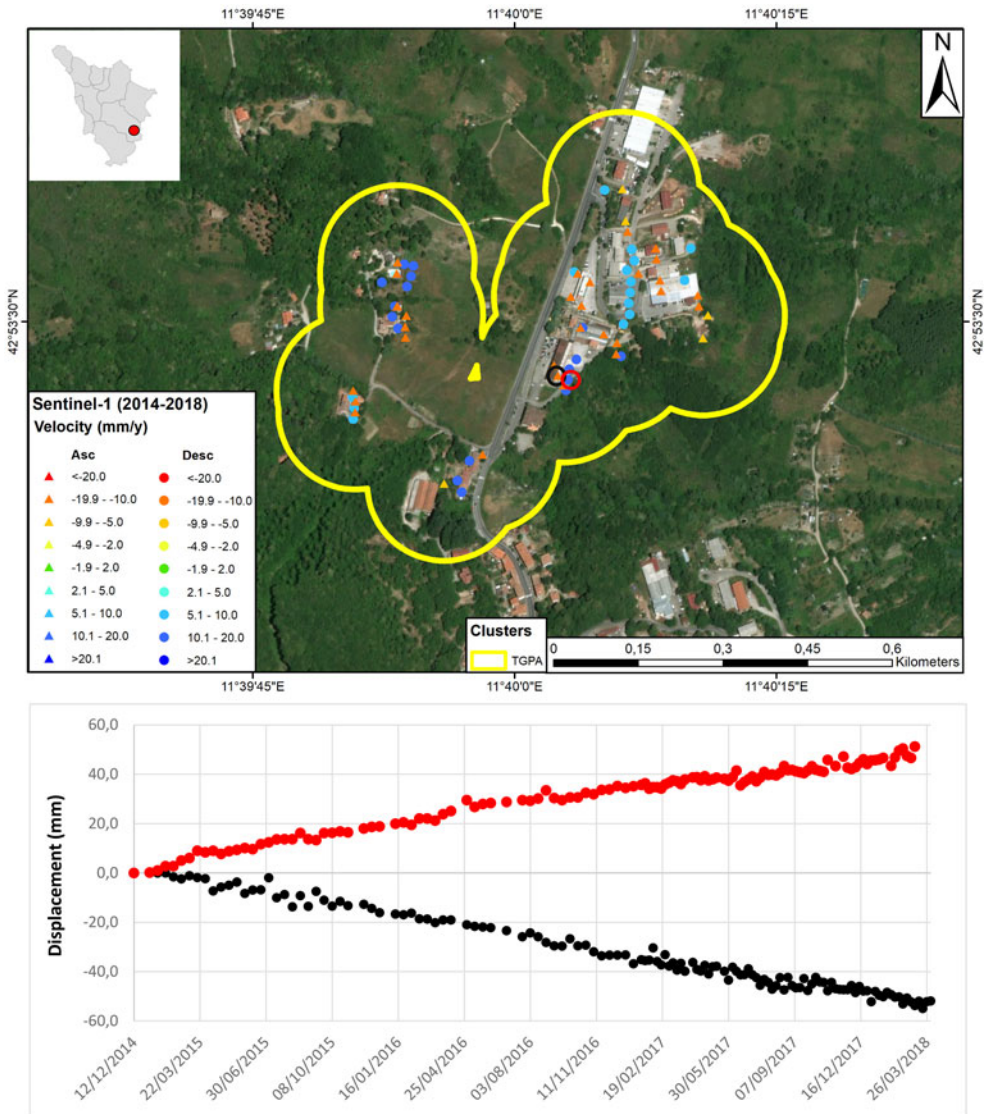
Figure 6. Example of TGPA Abbadia San Salvatore (SI) affected by landslides phenomena. The PS/DS data correspond to the period from October 2014 to April 2018. The black and the red circles indicate the PS points from which time series were extracted. Source: Author

Landslides Activity Index (LAI), which is the ratio between the number of active landslides and the total number of landslides, in order to highlight the municipalities with the higher critical level. Figure 7b shows the municipalities where the landslide's state of activity is changed, and where new landslides are found thanks to the analysis of Sentinel-1 data. In 50 municipalities at least one landslide changed its SoA with respect to the IFFI database (already updated by means of ERS 1/2 and Envisat data) (Rosi et al. 2018) and 12 of these register the presence of potential "new detected" landslides. A total of 197 landslides have been updated from "dormant" to "stable".

Figure 7. (a) shows the municipalities classified based on Landslide Activity Index. (b) shows in red the municipalities where the landslides changed their state of activity in "active" and, in green, if there are also new landslides in municipalities' territories. Source: Author

5. Discussion

In this work, a "hot-spot" analysis at regional scale has been performed over the Tuscany Region to highlight relevant ground deformations such as landslides, subsidence and uplift, starting from large MTInSAR dataset updated three times. With this approach, it was possible summarising hundreds of thousands of points in single clusters, grouped into a geo-database containing interferometric parameters, geographical and geomorphological information, a brief evaluation of the possible triggering cause and information about the temporal evolution of moving areas.

A large number of geo-hazards affects Tuscany Region, in fact 117.000 landslides in the IFFI inventory and $1094 \, km^2$ of subsidence areas are mapped. Therefore, it is important to create priority list of the main active phenomena on the territory, in order to help the local administrator to correctly allocate funds and plan proper remedial actions.

In this work, we do not carry out a simple clusters analysis of a single deformation map, but rather a comparison among three several periods: (i) the first one from October 2014 to April 2017, (ii) the second one from October 2014 to October 2017, (iii) the third one from October 2014 to April 2018. In this way, it was possible to study the spatial and temporal evolution of the deformation clusters, updated every six months starting from the first period, and to detect the most significant ones. In fact, although the clusters are extracted from deformation maps elaborated over a

long period, sometimes they may represent unrepresentative episodic phenomena (14% of the total). In addition, the TGPAs, which represent the overlapping clusters detected in different periods and acquisition geometries, have been defined. These areas provide an idea about the persistence of the motions, highlighting the most enduring and representative areas affected by geohazards.

The analysis of the three periods points out a decreasing trend of PS/DS density and as a consequence a decrease of the spatial distribution of the clusters. LOS velocity values register a little decrease as well. On one side, this is probably due to the increase of radar images used during the processing phase, along the three analysis periods, which improve the accuracy of the output data. On the other side, the absence of intense rainfall periods during the monitored period caused a long-term reduction of landslides motion, determining some of the cluster of the first period to fall outside the fixed moving threshold.

The cluster database, obtained every six months, can be a reliable tool for updating the geo-hazard inventories. In fact, it was possible to easily update the regional landslide database, checking the actual state of activity of the landslides. The result does not report new areas affected by subsidence, nevertheless this methodology may ensure the mapping of new phenomena in the future. Detecting new areas affected by subsidence, potentially connected with excessive exploitation of the ground-water, can play a role key for the water source managing as well.

6. Conclusion

In this work, we exploited Sentinel-1 images for active moving areas detection at regional scale. The study area is Tuscany Region, located in central Italy and characterized by an extremely variegated landscape with different geohazards, ranging from landslides to subsidence.

A hotspot-like methodology is proposed, exploiting the temporal repetitiveness of Sentinel-1 data analysed by means of the SqueeSAR algorithm to create deformation maps in three different periods with a six months update. Thanks to a filtering approach based on a velocity threshold, it was possible to extract a total of 652 deformation clusters, divided into three different periods, to study their spatial and temporal evolution. The final output is a flexible geo-database that contains interferometric parameters, geographical, geomorphological and geological information, a brief evaluation of the possible triggering cause and information about the temporal evolution of the moving areas. Considering the 6-days repeatability of the Sentinel-1 constellation, this clustering methodology turns out to be reliable, fast and readily reproducible.

This work represents the first cluster database in Tuscany region, focused on landslide and subsidence phenomena, required by regional Civil Protection for risk management. In fact, thanks to the update at regional scale it is possible to highlight the most important deformation areas and thus to create a priority list, allowing the reduction of economic and personnel costs and correctly planning countermeasures at municipal scale.

Disclosure statement

No potential conflict of interest was reported by the author(s).

Funding

ORCID

Lorenzo Solari 🆔 http://orcid.org/0000-0003-3637-2669
Silvia Bianchini 🆔 http://orcid.org/0000-0003-2724-5641
Matteo Del Soldato 🆔 http://orcid.org/0000-0001-7539-5850
Nicola Casagli 🆔 http://orcid.org/0000-0002-8684-7848

References

Abdikan S, Sanli FB, Ustuner M, Calò F. 2016. Land cover mapping using Sentinel-1 SAR data. Int Arch Photogramm Remote Sens Spatial Inf Sci. 41:757.

Aschbacher J, Milagro-Pérez MP. 2012. The European Earth monitoring (GMES) programme: status and perspectives. Remote Sens Environ. 120:3–8.

Barra A, Monserrat O, Mazzanti P, Esposito C, Crosetto M, Scarascia Mugnozza G. 2016. First insights on the potential of Sentinel-1 for landslides detection. Geomat, Nat Hazards Risk. 7(6):1874–1883.

Barra A, Solari L, Béjar-Pizarro M, Monserrat O, Bianchini S, Herrera G, Crosetto M, Sarro R, González-Alonso E, Mateos R, et al. 2017. A methodology to detect and update active deformation areas based on Sentinel-1 SAR images. Remote Sens. 9(10):1002.

Batini F, Brogi A, Lazzarotto A, Liotta D, Pandeli E. 2003. Geological features of Larderello-Travale and Mt. Amiata geothermal areas (southern Tuscany, Italy). Episodes 26(3): 239–244.

Bianchini S, Cigna F, Righini G, Proietti C, Casagli N. 2012. Landslide hotspot mapping by means of persistent scatterer interferometry. Environ Earth Sci. 67(4):1155–1172.

Bianchini S, Raspini F, Ciampalini A, Lagomarsino D, Bianchi M, Bellotti F, Casagli N. 2017. Mapping landslide phenomena in landlocked developing countries by means of satellite remote sensing data: the case of Dilijan (Armenia) area. Geomat., Nat. Haz. Risk. 8(2): 225–241.

Bortolotti V. 1992. The Tuscany–Emilian Apennine. Regional geological guidebook, Vol. 4, SGI BEMA Editrice, 329pp, Milan, Italy

Brogi A. 2008. The structure of the Monte Amiata volcano-geothermal area (Northern Apennines, Italy): Neogene-Quaternary compression versus extension. Int J Earth Sci (Geol Rundsch). 97(4):677–703.

Calamai A, Cataldi R, Squarci P, Taffi L. 1970. Geology, geophysics and hydrogeology of the Monte Amiata geothermal field. Geothermics 1(Spec):1–9.

Capecchi F, Guazzone G, Pranzini G. 1975. Il bacino lacustre di Firenze-Prato-Pistoia; geologia del sottosuolo e ricostruzione evolutiva. B Soc Geol Ital. 94(4):637–660.

Colombo D, Farina P, Moretti S, Nico G, Prati C. 2003. Land subsidence in the Firenze-Prato-Pistoia basin measured by means of spaceborne SAR interferometry. In Geoscience and

Remote Sensing Symposium, 2003. IGARSS'03. Proceedings. 2003 IEEE International (Vol. 4, 2927–2929). IEEE. Toulouse, France

Coltorti M, Brogi A, Fabbrini L, Firuzabadì D, Pieranni L. 2011. The sagging deep-seated gravitational movements on the eastern side of Mt. Amiata (Tuscany, Italy). Nat Haz. 59(1): 191–208.

Dai K, Li Z, Tomás R, Liu G, Yu B, Wang X, Cheng H, Chen J, Stockamp J. 2016. Monitoring activity at the Daguangbao mega-landslide (China) using Sentinel-1 TOPS time series interferometry. Remote Sens Environ. 186:501–513.

Del Soldato M, Bianchini S, Calcaterra D, De Vita P, Martire DD, Tomás R, Casagli N. 2017. A new approach for landslide-induced damage assessment. Geom, Nat Haz Risk. 8(2): 1524–1537.

Del Soldato M, Farolfi G, Rosi A, Raspini F, Casagli N. 2018. Subsidence evolution of the Firenze–Prato–Pistoia Plain (Central Italy) combining PSI and GNSS data. Remote Sens. 10(7):1146.

Del Soldato M, Riquelme A, Bianchini S, Tomàs R, Di Martire D, De Vita P, Moretti S, Calcaterra D. 2018. Multisource data integration to investigate one century of evolution for the Agnone landslide (Molise, southern Italy). Landslides 15(11):2113–2128.

Farina P, Casagli N, Ferretti A. 2007. Radar-interpretation of InSAR measurements for landslide investigations in civil protection practices. First North American landslide conference (272–283), Vail, Colorado, USA.

Faunt CC, Sneed M, Traum J, Brandt JT. 2016. Water availability and land subsidence in the Central Valley, California, USA. Hydro Jou. 24(3):675–684.

Ferretti A, Prati C, Rocca F. 2001. Permanent scatterers in SAR interferometry. IEEE Trans Geosci Remote Sens. 39(1):8–20.

Ferretti A, Fumagalli A, Novali F, Prati C, Rocca F, Rucci A. 2011. A new algorithm for processing interferometric data-stacks: SqueeSAR. IEEE Trans Geosci Remote Sens. 49(9): 3460–3470.

Galloway DL, Burbey TJ. 2011. Regional land subsidence accompanying groundwater extraction. Hydrogeol J. 19(8):1459–1486.

Gianelli G, Puxeddu M, Batini F, Bertini G, Dini I, Pandeli E, Nicolich R. 1988. Geological model of a young volcano-plutonic system: the geothermal region of Monte Amiata (Tuscany, Italy). Geothermics 17(5/6):719–734.

Herrera G, Fernández MÁ, Tomás R, González-Nicieza C, López-Sánchez JM, Vigil AÁ. 2012. Forensic analysis of buildings affected by mining subsidence based on Differential Interferometry (Part III.). Eng Failure Anal. 24:67–76.

Herrera G, Mateos RM, García-Davalillo JC, Grandjean G, Poyiadji E, Maftei R, Filipciuc T-C, Jemec Auflič M, Jež J, Podolszki L, et al. 2018. Landslide databases in the geological surveys of. Europe Landslides 15(2):359–379.

Hu R, Wang S, Lee C, Li M. 2002. Characteristics and trends of land subsidence in Tanggu, Tianjin, China. Bull Eng Geol Environ. 61(3):213–225.

Hu RL, Yue ZQ, Wang LU, Wang SJ. 2004. Review on current status and challenging issues of land subsidence in China. Engi Geol. 76(1–2):65–77.

Intrieri E, Raspini F, Fumagalli A, Lu P, Del Conte S, Farina P, Allievi J, Ferretti A, Casagli N. 2018. The Maoxian landslide as seen from space: detecting precursors of failure with Sentinel-1 data. Landslides 15(1):123–133.

Kvam PH, Vidakovic B. 2007. Nonparametric statistics with applications to science and engineering (Vol. 653).Hoboken, New Jersey :John Wiley & Sons.

Manzella A, Bonciani R, Allansdottir A, Botteghi S, Donato A, Giamberini S, Lenzi A, Paci M, Pellizzone A, Scrocca D. 2018. Environmental and social aspects of geothermal energy in Italy. Geothermics 72:232–248.

Massonnet D, Feigl KL. 1998. Radar interferometry and its application to changes in the Earth's surface. Rev Geophys. 36(4):441–500.

Ng AHM, Ge L, Du Z, Wang S, Ma C. 2017. Satellite radar interferometry for monitoring subsidence induced by longwall mining activity using Radarsat-2, Sentinel-1 and ALOS-2 data. Int J Appl Earth Observ. 61:92–103.

Peel MC, Finlayson BL, McMahon TA. 2007. Updated world map of the Köppen-Geiger climate classification. Hydrol Earth Syst Sci Discuss. 4(2):439–473.

Plank S. 2014. Rapid damage assessment by means of multi-temporal SAR—A comprehensive review and outlook to Sentinel-1. Remote Sens. 6(6):4870–4906.

Rapetti F, Vittorini S. 1994. Rainfall in Tuscany: observation about extreme events. Riv Geogr Ital. 101:47–76.

Raspini F, Bianchini S, Ciampalini A, Del Soldato M, Solari L, Novali F, Del Conte S, Rucci A, Ferretti A, Casagli N. 2018. Continuous, semi-automatic monitoring of ground deformation using Sentinel-1 satellites. Sci Rep. 8(1): 1–11

Rosi A, Segoni S, Catani F, Casagli N. 2012. Statistical and environmental analyses for the definition of a regional rainfall threshold system for landslide triggering in Tuscany (Italy). J Geograph Sci. 22(4):617–629.

Rosi A, Tofani V, Agostini A, Tanteri L, Stefanelli CT, Catani F, Casagli N. 2016. Subsidence mapping at regional scale using persistent scatters interferometry (PSI): The case of Tuscany region (Italy). Int J Appl Earth Observ. 52:328–337.

Rosi A, Tofani V, Tanteri L, Stefanelli CT, Agostini A, Catani F, Casagli N. 2018. The new landslide inventory of Tuscany (Italy) updated with PS-InSAR: geomorphological features and landslide distribution. Landslides 15(1):5–19.

Solari L, Barra A, Herrera G, Bianchini S, Monserrat O, Béjar-Pizarro M, Crosetto M, Sarro R, Moretti S. 2018. Fast detection of ground motions on vulnerable elements using Sentinel-1 InSAR data. Geomat, Nat Haz Risk. 9(1):152–174.

Solari L, Del Soldato M, Bianchini S, Ciampalini A, Ezquerro P, Montalti R, Raspini F, Moretti S. 2018. From ERS 1/2 to Sentinel-1: subsidence monitoring in Italy in the last two decades. Front Earth Sci. 6:149.

Solari L, Raspini F, Del Soldato M, Bianchini S, Ciampalini A, Ferrigno F, Tucci S, Casagli N. 2018. Satellite radar data for back-analyzing a landslide event: the Ponzano (Central Italy) case study. Landslides 15(4):773–782.

Sowter A, Amat MBC, Cigna F, Marsh S, Athab A, Alshammari L. 2016. Mexico City land subsidence in 2014–2015 with Sentinel-1 IW TOPS: Results using the Intermittent SBAS (ISBAS) technique. Int J Appl Earth Observ. 52:230–242.

Spizzichino D, Margottini C, Trigila A, Iadanza C, Linser S. 2010. Landslides. *Mapping the impacts of natural hazards and technological accidents in Europe. An overview of the last decade.* European Environment Agency EEA Technical Report 13 2010.

Stephens MA. 1970. Use of the Kolmogorov-Smirnov, Cramér-Von Mises and related statistics without extensive tables. J R Statist Soc. Ser B (Methodol). 32(1):115–122.

Tofani V, Segoni S, Agostini A, Catani F, Casagli N. 2013. Use of remote sensing for landslide studies in Europe. Nat Haz Earth Syst Sci. 13(2):299–309.

Torres R, Snoeij P, Geudtner D, Bibby D, Davidson M, Attema E, Potin P, Rommen BÖrn, Floury N, Brown M, et al. 2012. GMES Sentinel-1 mission. Remote Sens Environ. 120: 9–24.

Vai, F., & Martini, I. P. (Eds.). 2013. Anatomy of an orogen: the Apennines and adjacent Mediterranean basins.London, UK: Springer.

Vajedian S, Motagh M, Mousavi Z, Motaghi K, Fielding E, Akbari B, Wetzel H-U, Darabi A. 2018. Coseismic Deformation Field of the Mw 7.3 12 November 2017 Sarpol-e Zahab (Iran) Earthquake: A Decoupling Horizon in the Northern Zagros Mountains Inferred from InSAR Observations. Remote Sensing 10(10):1589.

van der Horst T, Rutten MM, van de Giesen NC, Hanssen RF. 2018. Monitoring land subsidence in Yangon, Myanmar using Sentinel-1 persistent scatterer interferometry and assessment of driving mechanisms. Remote Sens Environ. 217:101–110.

Wang H, Liu-Zeng J, Ng AH-M, Ge L, Javed F, Long F, Aoudia A, Feng J, Shao Z. 2017. Sentinel-1 observations of the 2016 Menyuan earthquake: A buried reverse event linked to the left-lateral Haiyuan fault. International J Appl Earth Observ. 61:14–21.

Zhang A, Lu J, Kim JW. 2018. Detecting mining-induced ground deformation and associated hazards using spaceborne InSAR techniques. Geomat, Nat Haz Risk. 9(1):211–223.